Cholesterol Depletion and Modification of COOH-Terminal Targeting Sequence of the Prion Protein Inhibit Formation of the Scrapie Isoform

Albert Taraboulos,* Michael Scott,* Andrew Semenov,* Dana Avraham,* Lajos Laszlo,* and Stanley B. Prusiner*‡

Departments of *Neurology and ‡Biochemistry and Biophysics, University of California, San Francisco, California 94143

Abstract. After the cellular prion protein (PrP^C) transits to the cell surface where it is bound by a glycophosphatidyl inositol (GPI) anchor, PrP^C is either metabolized or converted into the scrapie isoform (PrP^{Sc}). Because most GPI-anchored proteins are associated with cholesterol-rich membranous microdomains, we asked whether such structures participate in the metabolism of PrP^C or the formation of PrP^{Sc}. The initial degradation of PrP^C involves removal of the NH_2 terminus of PrP^C to produce a 17-kD polypeptide which was found in a Triton X-100 insoluble fraction. Both the formation of PrP^{Sc} and the initial degradation of PrP^C were diminished by lovastatin-mediated depletion of cellular cholesterol but were insensitive to NH_4Cl. Further degradation of the 17-kD polypeptide did occur within an NH_4Cl-sensitive, acidic compartment. Replacing the GPI addition signal with the transmembrane and cytoplasmic domains of mouse CD4 rendered chimeric $CD4PrP^C$ soluble in cold Triton X-100. Both $CD4PrP^C$ and truncated PrP^C without the GPI addition signal (Rogers, M., F. Yehieley, M. Scott, and S. B. Prusiner. 1993. *Proc. Natl. Acad. Sci. USA.* 90:3182–3186) were poor substrates for PrP^{Sc} formation. Thus, it seems likely that both the initial degradation of PrP^C to the 17-kD polypeptide and the formation of PrP^{Sc} occur within a non-acidic compartment bound by cholesterol-rich membranes, possibly glycolipid-rich microdomains, where the metabolic fate of PrP^C is determined. The pathway remains to be identified by which the 17-kD polypeptide and PrP^{Sc} are transported to an acidic compartment, presumably endosomes, where the 17-kD polypeptide is hydrolyzed and limited proteolysis of PrP^{Sc} produces PrP 27-30.

THE scrapie prion protein (PrP^{Sc})[1] is the only known component of the transmissible prion (Büeler et al., 1993; Prusiner, 1991; Prusiner et al., 1993) and is derived from a normal cellular protein (PrP^C) which is bound to the surface of cells by a glycophosphatidyl inositol (GPI) anchor (Stahl et al., 1987). In scrapie-infected cells in culture, PrP^{Sc} has been found to be derived from PrP^C molecules by a posttranslational process that involves a change in the conformation of PrP^C without evidence for chemical modification (Stahl et al., 1993). Spectroscopic studies have shown that PrP^C contains ~40% α-helix, and is devoid of β-sheet while PrP^{Sc} has more than 40% β-sheet (Pan et al., 1993; Safar et al., 1993). Upon conversion of PrP^C into PrP^{Sc}, prion protein (PrP) molecules acquire new biochemical and biophysical properties that can be used as markers for identification. Whereas PrP^C is readily soluble in most detergent and is completely degraded by proteases, PrP^{Sc} is insoluble in detergents, possesses a protease-resistant core termed PrP 27-30 (Meyer et al., 1986), and polymerizes into amyloid designated prion rods (Prusiner et al., 1983).

In scrapie-infected cells in culture, two mutually exclusive metabolic fates await plasma membrane PrP^C: (*1*) ~5% of PrP^C molecules are converted into PrP^{Sc} (Borchelt et al., 1990; Taraboulos et al., 1990*a*) and (*2*) >90% of PrP^C is degraded with a $t_{1/2}$ = ~6 h (Caughey et al., 1989). The subcellular sites for these two processes are unknown. The formation of PrP^{Sc} is thought to require direct interaction between PrP^C and existing PrP^{Sc} molecules (Kocisko et al., 1994; Prusiner et al., 1990). Nascent PrP^{Sc} is then NH_2-terminally trimmed in an acidic compartment (Caughey et al., 1991; Taraboulos et al., 1992) and accumulates within

Please address all correspondence to Dr. S. B. Prusiner, Department of Neurology, HSE-781, University of California, San Francisco, CA 94143-0518. Tel.: (415) 476-4482. Fax: (415) 476-8386.

The current address of Dr. Taraboulos is The Hebrew University-Hadassah Medical School, P. O. B. 11772, Jerusalem 91010, Israel. Tel.: 972 2 757086. Fax: 972 2 784010.

The current address of Dr. Lazlo is Department of General Zoology, Eotvos University, Budapest VIII., Puskin u. 3., H-1088, Hungary.

1. *Abbreviations used in this paper*: Ab, antibody; BFA, brefeldin A; GdnSCN, guanidine thiocyanate; GPI, glycophosphatidyl inositol; HaB, hamster brain; MF-DME, methionine free DME16 medium; Mo, mouse; N_2a, neuroblastoma; PIPLC, phosphatidylinositol-specific phospholipase C; PM, plasma membrane; PrP, prion protein; PrP^C, cellular isoform of the prion protein; PrP^{Sc}, scrapie isoform of the prion protein; Sarkosyl, sodium sarcosinate; ScN_2a, scrapie-infected neuroblastoma; SHa, Syrian hamster; wt, wild-type.

secondary lysosomes (McKinley et al., 1991; Taraboulos et al., 1990*b*). Uninfected cells do not produce PrP^{Sc}.

Since understanding the metabolism of PrP^{C} is important in the study of prions, we have explored the influence of its GPI anchor on the two alternative metabolic fates described above. GPI moieties are emerging as powerful sorting and targeting signals that direct proteins to specialized domains of the plasma membrane (PM) in various cell types. In particular, GPI-anchored proteins seem to be directed to a membrane microenvironment (Simons and van Meer, 1988) that renders them insoluble in cold Triton X-100 (Brown and Rose, 1992; Cerneus et al., 1993; Cinek and Horejsi, 1992; Hooper and Bashir, 1991). Detergent insolubility is acquired in the Golgi apparatus and appears to remain a property of these proteins throughout their lifetime. When this property is lost during turnover processes is unknown. While the exact nature of these Triton X-100 insoluble membrane domains is unknown, they are thought to be considerably enriched in cholesterol and sphingolipids (Brown and Rose, 1992).

Caveolae seem either to constitute a structurally and functionally specialized subset of the Triton X-100 insoluble membrane domains, or to associate closely with them (Anderson et al., 1992). In cells possessing caveolae, the folate receptor, PrP^{C} and other GPI-anchored proteins cluster in the vicinity of these PM invaginations (Ying et al., 1992). However, the immunoelectron microscopic and the immunofluorescence data supporting this caveolar clustering have recently been criticized on the ground that antibody cross-linking was responsible for some of this clustering (Mayor et al., 1994). Cholesterol is necessary both for the structural integrity of caveolae and their only currently known function, folate potocytosis (Anderson et al., 1992; Anderson, 1993; Chang et al., 1992; Rothberg et al., 1990*b*). In one study, caveolae were identified on the surface of neuroblastoma (N_2a) cells and quantitative immunocytochemistry of PrP^{C} revealed numerous clusters of gold particles on the surfaces of these cells, 12% of which were in caveolae (Ying et al., 1992). In contrast, other investigators failed to identify caveolae in N_2a cells (Shyng et al., 1994).

Because there is disagreement about morphologically defined caveolae in N_2a cells, our studies focused on membrane microdomains defined operationally by their insolubility in Triton X-100 (Brown and Rose, 1992). In addition to measuring the Triton X-100 insolubility of PrP^{C} and its degradation products, we examined the cholesterol deprivation of cells and replacement of the GPI anchor of PrP with a transmembrane sequence. Upon analyzing the turnover of PrP^{C}, we unexpectedly found that degradation occurs in two distinct steps. First, the polypeptide is NH_2-terminally clipped resulting in a 17-kD polypeptide (unglycosylated M_r) similar, or possibly identical, to PrP^{C}-II first identified in Syrian hamster (SHa) brain (Haraguchi et al., 1989; Pan et al., 1992). This degradative step occurs within Triton X-100 insoluble domains. Second, the 17-kD fragment was completely degraded within an acidic compartment which is likely to be endosomal. When cells were depleted of cholesterol, PrP^{C} degradation was slowed, and the generation of PrP^{Sc} molecules was inhibited. Under these conditions, the synthesis of PrP^{C} proceeded normally or was even increased.

To examine the importance of the GPI anchoring of PrP, we replaced the GPI addition signal with the transmembrane and cytoplasmic regions of mouse CD4 (Littman and Gettner, 1987) that target proteins to clathrin-coated pits (Keller et al., 1992). In contrast to GPI-anchored PrP^{C}, chimeric CD4PrP expressed in ScN_2a cells was equally soluble in Triton X-100 at 4°C and 37°C and was not converted into PrP^{Sc}. Deletion of the GPI addition signal at the COOH terminus of PrP was previously found to diminish but not abolish PrP^{Sc} synthesis in scrapie-infected neuroblastoma (ScN_2a) cells (Rogers et al., 1993). In addition, a patient with Creutzfeldt-Jakob disease has been identified who has an amber mutation at codon 145 resulting in the translation of truncated, anchorless PrP molecules some of which formed PrP amyloid plaques (Kitamoto et al., 1993). Thus, the GPI anchor seems to be dispensable for the structural changes which occur during the formation of PrP^{Sc}.

The foregoing results suggest that a cholesterol-dependent pathway related to the membrane microenvironment of PrP^{C} is involved in the degradation of PrP^{C} and in the formation of PrP^{Sc}.

Materials and Methods

Materials

Cholesterol standard (965-25), lipid-cholesterol rich supplements (L 4848), and mevalonic acid lactone (M 9627) were from Sigma Chem. Co. (St. Louis, MO). Lovastatin (a generous gift from Merck, Sharp, and Dohme research laboratories, West Point, PA) was saponified (Langan and Volpe, 1986) before use. [^{35}S]Methionine was from New England Nuclear (Boston, MA). Reduced lipid FBS was first purchased from Sigma Chem. Co. (F 8895). When this product was discontinued we prepared reduced lipid FBS (Goldstein et al., 1983). Reagents for cell culture were purchased from the University of California San Francisco Cell Culture Facility (San Francisco, CA), except the methionine-free medium and the G418 which were from GIBCO BRL (Gaithersburg, MD). Tunicamycin and phosphatidylinositol-specific phospholipase C (PIPLC) (*B. Cereus*) were from Boehringer Mannheim Corp. (Indianapolis, IN). Protein A–Sepharose was from Pharmacia Biotech (Piscataway, NJ). All other chemicals and inhibitors were from Sigma Chem. Co.

Cultured Cells

N_2a cells were obtained from the Amer. Tissue Culture Collection (Rockville, MD). ScN_2a cells are the persistently infected clone as described (Butler et al., 1988). Hamster brain (HaB) cells were derived from the culture of a Syrian hamster (SHa) brain as described (Taraboulos et al., 1990*a*). ScN_2a-MHM2 expressing the gene PrP-MHM2 were as described (Scott et al., 1992). All the cells were grown and maintained at 37.5°C in DME16 supplemented with 10% FBS, except when specified otherwise. Cells transfected with CD4PrP in the pSPOX vector were grown in the same medium supplemented with 1 g/ml G418. Cells for the lovastatin experiments were set up according to the following standard format unless otherwise specified: On day zero, $\sim 1.5 \times 10^6$ cells were seeded on 6-cm plates (Corning Glass Works, Corning, NY), and grown for 2 d in regular medium. On day 2, the medium was replaced by fresh DME supplemented in some cases with 10% reduced lipid FBS (Goldstein et al., 1983) and 200 μM mevalonate. When needed, lovastatin was added to 0.3 μM on day 2. On day 5, the medium was replaced with fresh medium containing identical supplements. The experiments were carried out on day 6, except when specified otherwise.

Antibodies

R073 is an antiserum raised in a rabbit against SDS-PAGE purified SHaPrP 27-30 which reacts with SHaPrP, mouse (Mo) PrP, and MHM2PrP (Serban et al., 1990; Taraboulos et al., 1990*b*). 3F4 is a mAb raised against SHaPrP 27-30 (Kascsak et al., 1987). Its epitope, (Met_{109}-Met_{112}) is present on SHa as well as on MHM2PrP, but not on the MoPrP gene (Rogers et al., 1992). Thus, the 3F4 mAb does not recognize the wild-type (wt) MoPrP in ScN_2a cells but reacts with the products of the chimeric PrP genes MHM2PrP (Scott et al., 1992) and MHM2-CD4PrP. The mAb 13A5 was

raised against SHaPrP 27-30 (Barry and Prusiner, 1986). Anti P1, anti P5, and anti P3 are monospecific rabbit sera raised against the SHaPrP peptides 90-102, 142-174, and 220-233, respectively.

Metabolic Radiolabeling and Inhibitors

Confluent cells growing on 5-cm plates were rinsed three times with PBS and incubated for 30 min with methionine free DME16 medium (MF-DME). The medium was then replaced with fresh MF-DME supplemented with 0.5 mCi of [^{35}S] L-methionine (New England Nuclear, Boston, MA) supplemented with 5% of the appropriate serum as indicated in each experiment. At the end of the labeling period, the cells were rinsed twice with ice-cold PBS, and then either lysed and processed for immunoprecipitation or chased in DME plus 10% FCS for the appropriate length of time. When needed, mevalonate was added throughout the pulse and chase. Inhibitors were added either to the pulse or the chase periods, or both, as necessary. Inhibitors used in the pulse period were also added to the methionine starvation period.

Tunicamycin (5 mg/ml in DMSO) was freshly prepared for each experiment. Lovastatin was solubilized in EtOH, and then saponified with NaOH before its solubilization in water. Mevalonate was dissolved in EtOH at 4 μg/ml and stored at −20°C.

Triton X-100 Solubility Assay

Assays for solubility in Triton X-100 were performed on ice in a cold room (~4°C). Cells growing on 5-cm plates were rinsed twice with ice-cold PBS, chilled on ice for 15 min, and then lysed with 1-ml ice-cold Triton X-100 lysis buffer (1% Triton X-100, 150 mM NaCl, 10 mM Tris-HCl, pH 7.8) for 10 min. The lysates were then split into two equal fractions and transferred to 1.5-ml centrifugation tubes; one half was incubated at 37°C for 5 min while the other half was kept on ice. In some cases, aliquots of lysates were incubated with saponin (to a final concentration of 1%) for 10 min on ice before ultracentrifugation. The lysates were then centrifuged at 30,000 rpm (39,000 *g*) for 30 min in a TLA 100.3 rotor (Beckman Instrs., Fullerton, CA) at 2°C. The supernatant was then processed for immunoprecipitation (see next section) after the addition of sodium sarcosinate (Sarkosyl) (1% (vol/vol) final concentration). The pellets of the high speed centrifugation were discarded.

We found that prolonged ultracentrifugation was necessary to sediment quantitatively the Triton X-100 insoluble PrP^C; this contrasts with work of others using different cells and assaying for Triton X-100 insolubility of different GPI-proteins (Brown and Rose, 1992). Possible reasons for differences in sedimentation of GPI-proteins in cold Triton X-100 are discussed in the Results section. Since Triton X-100 insoluble PrP^C could be detected only when the temperature of the lysates was kept under 4°C at all times, it was essential to perform the procedure on ice in the cold room.

Cell Lysis and Immunoprecipitation

The cells were processed for immunoprecipitation as described elsewhere (Taraboulos et al., 1992) with some modifications. Cells growing on 5-cm plates were lysed in cold lysis buffer (100 mM NaCl, 10 mM EDTA, 0.5% NP-40, 0.5% sodium deoxycholate, 10 mM Tris-HCl, pH 7.8); this lysis was performed at room temperature and the insoluble material was removed by a low-speed centrifugation for 10 s in an Eppendorf centrifuge at room temperature. Sarkosyl, PMSF and the relevant antiserum were added to final concentrations of 1%, 0.1 M, and 1 μl/ml, respectively, for immunoprecipitation of PrP^C. For the purification of PrP^{Sc}, the lysates were digested with proteinase K before guanidine thiocyanate (GdnSCN) denaturation and methanol precipitation. The methanol pellets were resuspended in 1 ml TNS (100 mM NaCl, 1% Sarkosyl, 10 mM Tris-HCl, pH 7.8); supplemented with 0.1 mM PMSF for immunoprecipitation.

When needed, PrP^C was separated from PrP^{Sc} by ultracentrifugation before immunoprecipitation. 1% Sarkosyl and 0.1 M PMSF were added to the lysate that was then centrifuged at 39,000 *g*, 1 h in a Beckman TL-100 centrifuge equipped with a TLA-100.3 rotor to remove PrP^{Sc} (Meyer et al., 1986), and the supernatant was used for immunopurification. The antibody (Ab) was then incubated overnight at 4°C. Protein A-Sepharose beads were then added to the lysate for a 1-h incubation at room temperature, and the immunoadsorbed proteins were purified by rinsing in TNS buffer. Protein A-Sepharose was used for all the rabbit sera as well as for 3F4, which binds well protein A. For 13A5, an additional incubation step with rabbit anti-mouse IgG serum (Sigma Chem. Co.) was added before the precipitation with protein A.

SDS-PAGE and Autoradiography

The immunopurified proteins were analyzed on 12% SDS acrylamide gels as previously described (Laemmli, 1970). Radiolabeled proteins were detected by autoradiography on AR X-ray films (Kodak). In some cases, the radioactivity in the gels was quantified using a PhosphorImager from Molecular Dynamics (San Diego, CA).

Cholesterol and Protein Determination

Cells were lysed in lysis buffer, and 20 μl of the postnuclear supernatant was used for the fluorogenic reaction which measures free cholesterol (Heider and Boyett, 1978). The system was calibrated using a cholesterol calibration solution from Sigma Chem. Co. Excitation was at 325 nm and emission was monitored between 315 nm and 500 nm. Fluorescence was assayed in a spectrofluorimeter model LS 50 B (Perkin Elmer Corp., Norwalk, CT). Total protein content of the cells was determined using the BCA kit from Pierce (Rockford, IL).

Recombinant MHM2-CD4PrP Gene

To construct the MHM2-CD4PrP, the transmembrane and cytoplasmic regions of CD4 (Littman and Gettner, 1987) were fused to the MHM2PrP-(del 231-254) gene lacking the GPI attachment sequence (Rogers et al., 1993). First, PvuI and XhoI restriction sites were introduced in the CD4 sequence by PCR using the mismatched primers CD1 (5′ A GGG GTG AAC CGA TCG GTG TTC CTG GCT) resulting in the mutations Gln_{367}→Arg and Thr_{368}→Ser, and CD2 (5′ CTC ATC TGA GGC CTC GAG CCA CCT GCA) (the mismatched nucleotides are underlined). The polymerase chain reaction fragment was then restricted with PvuI and XhoI and ligated into the MHM2PrP(del 231-254), yielding with MHM2-CD4PrP sequence, which was then introduced into the expression plasmid pSPOX (Scott et al., 1992) at the unique sites BglII and XhoI. MHM2-CD4PrP is referred to as CD4PrP throughout this article.

N_2a and SCN_2a cells were transfected with pSPOX-CD4PrP using lipofectin (GIBCO BRL) used according to the manufacturer's instructions, and they were then selected and maintained with 1 mg/ml of G418.

Western Blotting

In some cases, PrP^{Sc} from cells was concentrated by limited proteolysis followed by ultracentrifugation before Western blot analysis. This permitted the loading of an entire 9-cm plate-equivalent per lane of the SDS-PAGE, resulting in an increase in the sensitivity of PrP^{Sc} detection. One ml of lysis buffer was added to the cells on a 9-cm plate and the postnuclear supernatant was digested with proteinase K (50 μg/ml, 37°C, 1 h). Sarkosyl and PMSF were added to final concentrations of 1% and 0.1 mM, respectively, and the samples centrifuged at 57,000 *g*, 1 h, 4°C. The pellets were solubilized in 100 μl containing 3 M of GdnSCN and 1% Sarkosyl; after incubating the samples at 65°C for 5 h, the GdnSCN was then removed by EtOH precipitation before loading the SDS-PAGE.

Immunofluorescence

For the immunofluorescent detection of cell surface PrP, cells growing on Permanox slides (Nunc, Inc., Naperville, IL) were incubated with the relevant Ab (1:50 of either antiserum or ascitic fluid) for 2 h at 4°C in PBS supplemented with reduced lipid FBS. For detection of MoPrP endogenous to the N_2a cells, we used the rabbit antiserum R073. For the detection of CD4PrP, we used the mAb 3F4 (Kascsak et al., 1987) ascitic fluid. After rinsing with ice-cold PBS, the cells were fixed (10% formalin in PBS, 4°C, 30 min), in appropriate cases permeabilized (0.1% Triton X-100, RT, 5 min), and incubated for 30 min in 1% NH_4Cl in PBS to quench the aldehydes. The cells were then blocked in 5% milk in PBS, incubated with a fluorescein isothiocyanate-labeled anti-rabbit or anti-mouse IgG for 3F4 and R073, respectively, for 30 min under the same conditions as the primary Ab, rinsed, and finally mounted in propyl gallate (Giloh and Sedat, 1982).

Results

Metabolism and Degradation of PrP^C

The degradation of PrP^C and formation of PrP^{Sc} in ScN_2a cells are mutually exclusive fates experienced by plasma membrane PrP^C molecules. We first examined the turnover

of PrP^c and its possible association with Triton X-100 insoluble microdomains. To dissect the pathway of PrP^c degradation, we used pulse-chase radiolabeling experiments. ScN_2a cells were radiolabeled for 2 h, and then chased for the indicated period of time, and PrP^c (the detergent soluble PrP) was immunoprecipitated with the polyclonal antiserum R073 and analyzed by SDS-PAGE (Fig. 1 *A*). The 33–35-kD band was degraded with a $t_{1/2}$ of several hours, as previously described (Borchelt et al., 1990; Caughey et al., 1989). When NH_4Cl (40 mM) was added to the pulse and the chase media, a lower (M_r = 26–29 kD) band appeared after 2 h of chase (Fig. 1 *B*). The increase in the 26–29-kD band correlated with the decrease in the 33–35-kD band, suggesting that this lower band is a degradation product stabilized by NH_4Cl.

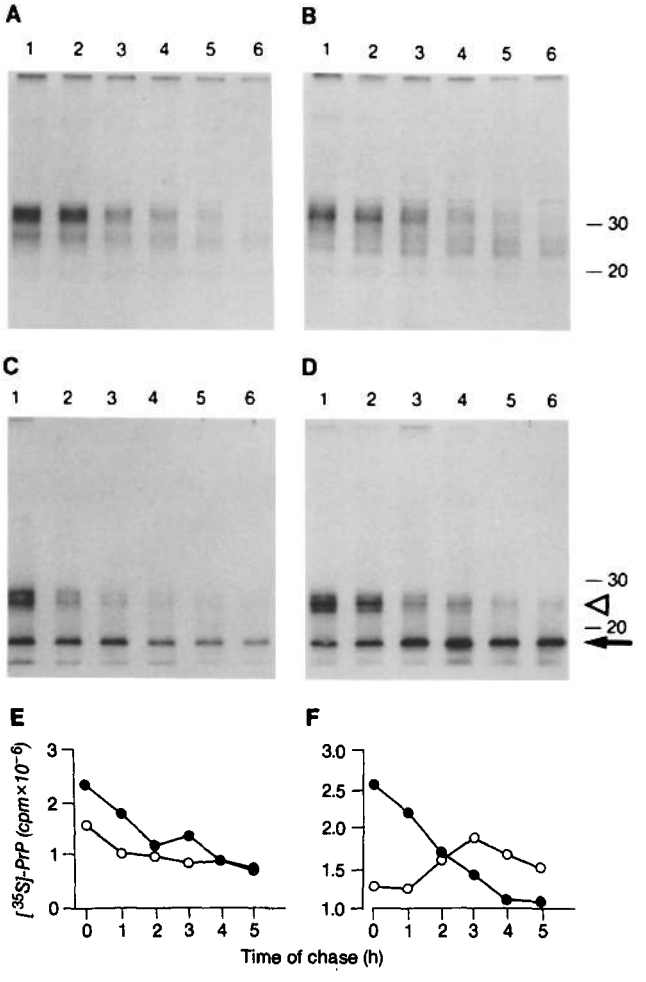

Figure 1. Degradation of PrP^c. (*A*) ScN_2a cells were radiolabeled for 2 h and chased for 0, 2, 4, 6, 10, or 24 h. (*B*) ScN_2a cells were both radiolabeled for 2 h and chased for the same times as in *A* in the presence of 40 μM NH_4Cl. After lysis, the cells were centrifuged at 57,000 *g* for 1 h at 4°C to sediment PrP^{Sc}. PrP^c was immunoprecipitated from the supernatant using the polyclonal R073 antiserum. (*C*) HaB cells were radiolabeled for 1 h in the presence of tunicamycin (5 μg/ml), and chased for 0, 1, 2, 3, 4, or 5 h. Cellular PrP^c was then immunoprecipitated with R073. The 17-kD band is marked by an arrow and the 26-kD band by an arrowhead. (*D*) NH_4Cl (40 μM) was added throughout the pulse and the chase. In the NH_4Cl-treated cells, the 17-kD degradation product (*arrow*) accumulated during longer chases. (*E*) Radioactivity in the PrP bands of HaB cells in *C* treated with tunicamycin quantified with a PhosphorImager scanner. (*F*) Radioactivity in the PrP bands of HaB cells in *D* treated with both tunicamycin and NH_4Cl. (*Closed circles*) 26 kD PrP. (*Open circles*) 17 kD PrP.

To reduce the heterogeneity in the M_r of the PrP bands, which obscured their identity, we used tunicamycin. In both ScN_2a cells (not shown) and SHa brain cells (Fig. 1, *C* and *D*), unglycosylated PrP^c was rapidly degraded to a 17-kD product (*arrow*). HaB cells were used in order to take advantage of the α-PrP mAbs and α-PrP peptide monospecific antisera (Barry et al., 1988; Rogers et al., 1991) in the mapping of this 17-kD degradation intermediate. HaB cells were radiolabeled for 1 h in the presence of 5 μM tunicamycin and chased for increasing periods of time ranging from 0 to 5 h (Fig. 1, *C* and *D*). Samples were lysed and PrP^c immunoprecipitated with R073 antiserum followed by SDS-PAGE. To ensure that all degradation fragments are detected, we initially used the R073 polyclonal antiserum which was raised against PrP 27-30 (Serban et al., 1990). The radioactivities in each of the PrP bands was quantified by phosphorimaging (Fig. 1, *E* and *F*). Unglycosylated PrP^c (the 25-kD band, *arrowhead*) was rapidly degraded while the 17-kD product (*arrow*) was degraded more slowly (Fig. 1, *C* and *E*). When NH_4Cl was added to both the pulse and chase periods, the 17-kD polypeptide increased with a concomitant decrease in the 26-kD band, suggesting a precursor-product relationship between these two PrP forms (Fig. 1, *D* and *F*). That NH_4Cl prevented the degradation of the 17-kD polypeptide is reminiscent of the inhibition by NH_4Cl of the NH_2-terminal digestion of PrP^{Sc} to form PrP 27-30 (Taraboulos et al., 1992). It seems likely that both the degradation of the 17-kD polypeptide and the production of PrP 27-30 occur in an acidic compartment of the endosomal pathway.

In ScN_2a cells not treated with tunicamycin (Fig. 1 *A*), the 26–29-kD degradation product probably corresponds to the unglycosylated 17-kD polypeptide. While NH_4Cl prevented degradation of the 17-kD polypeptide, the degradation of full-length PrP^c was similar whether or not NH_4Cl was present in the cell medium (Fig. 1, *B* and *D*). Scrapie infection did not alter the degradation of PrP^c as assessed in studies comparing uninfected N_2a and infected ScN_2a cells (not shown).

To map the 17-kD fragment, we used a panel of α-PrP peptide monospecific antisera and α-PrP mAbs directed against SHaPrP (Fig. 2 *A*). While the full-length 26-kD band (Fig. 2 *B*, *arrowhead*) was immunoprecipitated with all the Abs, the 17-kD degradation intermediate (*arrow*) reacted only with Abs directed against epitopes situated in the COOH-terminal portion of the molecule (Fig. 2 *B*) including epitope P3 at the COOH terminus of the mature protein. These results argue that the 17-kD product is generated by cleavage between the 3F4 and the 13A5 epitopes, i.e., between amino acids 111 and 138 of MoPrP or 112 and 139 of SHaPrP, and consists of the COOH-terminal portion of PrP^c (Fig. 2 *A*). A cleavage site in the corresponding region of the chicken PrP has been reported (Harris et al., 1993). We conclude that the first step in PrP^c degradation involves the hydrolysis of the ~90 NH_2-terminal residues which are removed in a NH_4Cl-insensitive process. The remaining 17-kD fragment is stabilized by NH_4Cl and its degradation is thus likely to take place in an acidic, presumably endocytic compartment. These results argue that the 17-kD polypeptide is

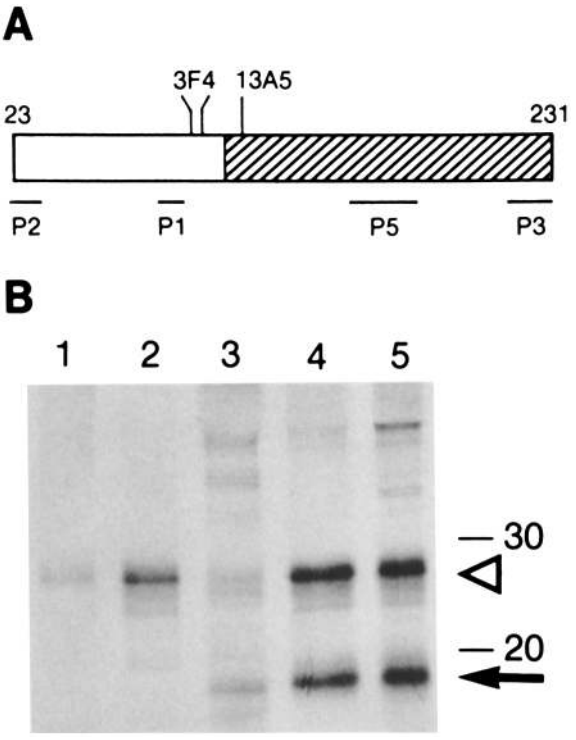

Figure 2. Characterization of the 17-kD degradative intermediate of PrP^C. (*A*) Linear map of SHaPrP showing the location of several epitopes. The hatched bar denotes the 17-kD intermediate identified in *B*. (*B*) HaB cells were labeled for 4 h with tunicamycin and NH_4Cl, and PrP^C was immunoprecipitated with the following Abs: αP1 (lane *1*), 3F4 (lane *2*), 13A5 (lane *3*), αP5 (lane *4*), and αP3 (lane *5*). The 17-kD band (*arrow*) reacted with 13A5, αP5, and αP3 but not with αP1 and 3F4, whereas the 26-kD band (*arrowhead*) reacted with all Abs.

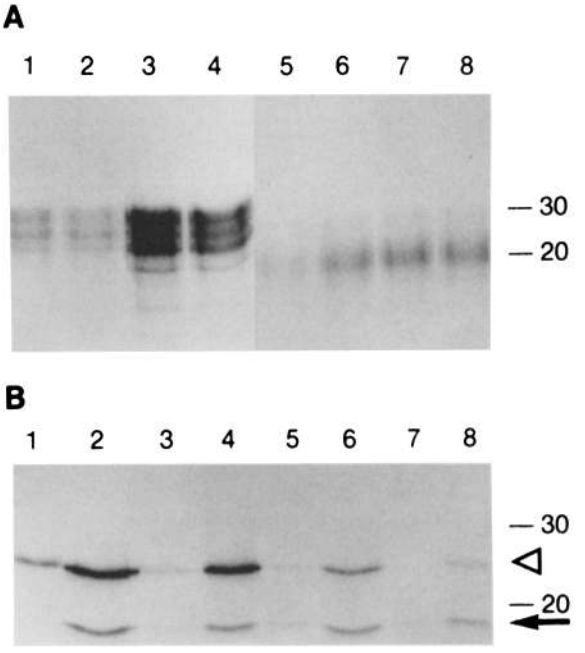

Figure 3. PrP^C degradation occurs within cholesterol-rich rafts. (*A*) ScN_2a cells were radiolabeled for 2 h. In lanes *5–8*, the cells were then chased in unlabeled medium for an additional 18 h. NH_4Cl (40 μM) was present during the pulse and the chase period. The cells were then lysed in 1% Triton X-100 at either 4°C (lanes *1*, *2*, *5*, and *6*) or 37°C (lanes *3*, *4*, *7*, and *8*). The lysates were centrifuged at 39,000 *g* for 1 h at either 2°C (cells lysed at 4°C) or at 25°C (cells lysed at 37°C). PrP was immunoprecipitated from the supernatant using R073 antiserum. (*B*) ScN_2a cells were radiolabeled for 1 h in the presence of tunicamycin (20 μM) and chased for 0, 1, 2, or 3 h. (lanes *1* and *2*, *3* and *4*, *5* and *6*, and *7* and *8*, respectively.) NH_4Cl (40 μM) was included during both the pulse and the chase periods. The cells were lysed in 1% Triton X-100 either at 4°C (*odd-numbered* lanes) or at 37°C (*even-numbered* lanes), centrifuged and analyzed as described for panel *A*.

the same as or very similar to the NH_2 terminally truncated PrP^C found in purified fractions from SHa brain which we earlier designated PrP^C-II (Haraguchi et al., 1989; Pan et al., 1992).

NH_2-Terminal Degradation of PrP^C Occurs within Triton X-100 Insoluble Domains

The removal of the NH_2 terminus of PrP^C is an important metabolic event since it probably renders PrP^C ineligible for conversion to PrP^{Sc}. To characterize the subcellular site of this proteolytic process, we analyzed the solubility of both the precursor and product after treatment with Triton X-100. ScN_2a cells treated with NH_4Cl (40 μM) were radiolabeled for 2 h, and then either harvested immediately (Fig. 3 *A*, lanes *1–4*) or chased in unlabeled medium (lanes *5–8*). The cells were lysed in 1% Triton X-100 either at 4°C (lanes *1*, *2*, *5*, and *6*) or at 37°C (lanes *3*, *4*, *7*, and *8*) and centrifuged at 39,000 *g* for 1 h at 2°C. PrP was immunoprecipitated from the supernatant using R073 antiserum. Both full-length PrP^C and the 17-kD degradation intermediate displayed similar differential solubility in Triton X-100 suggesting a similar membrane microenvironment for both these PrP species. To determine if similar results would hold for the unglycosylated PrP^C, we radiolabeled ScN_2a cells for 1 h in the presence of tunicamycin (Fig. 3 *B*), and then chased them for increasing periods of times ranging from 0 to 3 h. The cells were then extracted with 1% Triton X-100 at either 4°C or 37°C, spun as before, and PrP^C was immunoprecipitated from the supernatant. Both the 26-kD band (*arrowhead*) and the 17-kD band (*arrow*) were almost insoluble at 37°C suggesting their association with cholesterol-rich complexes. Using PIPLC, we also found that the degradation intermediate is GPI linked to membranes (data not shown).

The initial step in PrP^C degradation appears to take place within a Triton X-100 insoluble, presumably cholesterol-rich microenvironment. Whether PrP^{Sc} is also formed within a similar environment remains to be established. Sedimentation in cold Triton X-100 cannot be used to appraise the association of PrP^{Sc} with these microdomains, because PrP^{Sc} is insoluble in non-denaturing detergents (Meyer et al., 1986).

Lovastatin Diminishes PrP^C Degradation

To investigate the influence of cholesterol depletion on PrP^C degradation, we compared N_2a and ScN_2a cells treated either with or without 0.3 μM lovastatin for 4 d (Fig. 4). The cells were radiolabeled for 1 h in the presence of tunicamycin (20 μM), and PrP^C was immunopurified after increasing

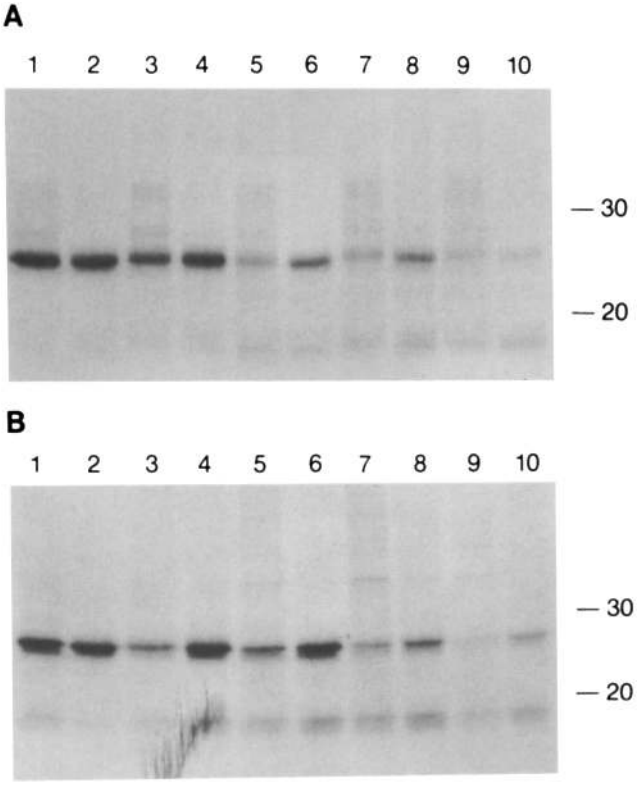

Figure 4. Slowed degradation of PrP^C for lovastatin-treated cells. (*A*) N_2a and (*B*) ScN_2a cells grown in reduced lipid medium without (*odd-numbered* lanes) or with lovastatin (0.3 μM) (*even-numbered* lanes) were pulse radiolabeled for 1 h in the presence of tunicamycin (20 μg/ml), and then chased for 0 (lanes *1* and *2*), 1 h (lanes *3* and *4*), 2 h (lanes *5* and *6*), 3 h (lanes *7* and *8*), or 4 h (lanes *9* and *10*). PrP^C was then immunoprecipitated and analyzed by SDS-PAGE.

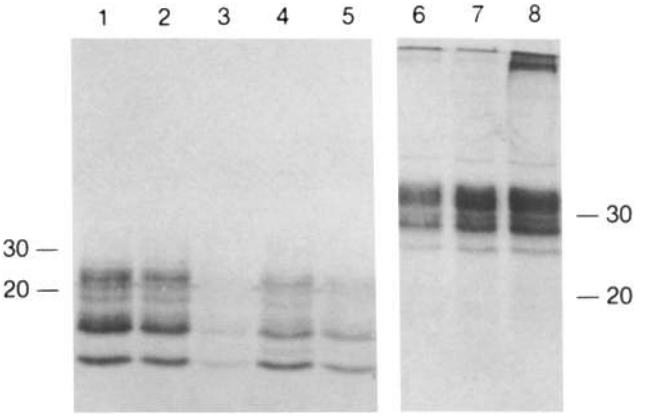

Figure 5. Lovastatin reduces PrP^{Sc} synthesis in ScN_2a cells. (Lanes *1–5* [Immunoblots]) ScN_2a cells were grown for 4 d with normal FBS (lane *1*), normal FBS and 0.3 μM lovastatin (lane *2*), reduced fat FBS and 0.3 μM lovastatin (lane *3*), reduced fat FBS (lane *4*), or reduced fat FBS and 0.3 μM lovastatin supplemented with 2.5 μg/ml cholesterol (lane *5*). They were then lysed, subjected to proteolysis catalyzed by proteinase K (50 μg/ml, 1 h, 37°C), and analyzed by SDS-PAGE. Western immunoblots were probed with the polyclonal Ab R073. PrP^{Sc} was reduced in cells treated with lovastatin in reduced fat serum when no exogenous cholesterol was added. (Lanes *6–8* [Autoradiographs]) PrP^C in ScN_2a cells were grown for 4 d with reduced fat serum. In lane *6*, no other chemical was added, whereas the cells in lane *7* were supplemented with lovastatin (0.3 μM), and in lane *8* both lovastatin (0.3 μM) and cholesterol (2.5 μg/ml) were added to the medium. The cells were then metabolically radiolabeled for 2 h, lysed, immunoprecipitated with R073, and analyzed by SDS-PAGE.

periods of chase ranging from 0 to 4 h and analyzed by SDS-PAGE. The rate of PrP^C degradation was reduced in the lovastatin-treated cells. Whether decreased degradation of PrP^C is a consequence of disrupting cholesterol-rich domains on the plasma membrane or results from a delayed export of PrP^C to the cell surface remains to be determined.

Lovastatin Reduces PrP^{Sc} Synthesis

Since lovastatin diminished the degradation of PrP^C, we determined whether depriving cells from cholesterol interfaces with the synthesis of PrP^{Sc}. ScN_2a cells were plated at low density (ca. 5×10^5 cells per 5-cm dish) in DME16 supplemented with lipid deficient FBS. Lovastatin was added at concentrations of 0.1, 0.3, 1, or 3 μM to inhibit cellular sterols synthesis; with the two highest lovastatin concentrations, cytopathology was considerable after 5 d. Cells were lysed and PrP^{Sc} analyzed by Western immunoblotting of proteinase K digested lysates. PrP^{Sc} content decreased with increasing lovastatin concentration (not shown). A concentration of 0.3 μM lovastatin was chosen for subsequent experiments because it reduced the amount of PrP^{Sc} while being only minimally cytopathic.

To explore the effect of cholesterol depletion on PrP^{Sc}, we incubated ScN_2a cells for 4 d in a variety of conditions: normal FBS (Fig. 5, lane *1*), normal FBS and 0.3 μM lovastatin (lane *2*), reduced lipid FBS and 0.3 μM lovastatin (lane *3*), reduced lipid FBS and lovastatin with the addition of cholesterol (2.5 μg/ml, lane *4*) and reduced lipid FBS (lane *5*). Mevalonate (200 μM) was included in the medium of all samples to provide for non-sterol pathways, such as protein isoprenylation. Western immunoblots showed that protease-resistant PrP^{Sc} was reduced in cells treated with lovastatin in the presence of reduced fat FBS (Fig. 5, lane *3*) in which cellular free cholesterol was reduced by 30%. Addition of cholesterol throughout the lovastatin treatment prevented the decrease in PrP^{Sc} (Fig. 5, lane *4*), arguing that the inhibition of PrP^{Sc} was caused by the depletion in cholesterol rather than in other mevalonate metabolites.

The synthesis of PrP^{Sc} in lovastatin-treated cells was also studied in pulse-chase metabolic radiolabeling experiments, in which cells were labeled for 2 h and chased for 7 h before PrP^{Sc} analysis (data not shown). These experiments also showed that PrP^{Sc} synthesis was reduced in lovastatin-treated cells. In contrast, PrP^C synthesis was unaltered by lovastatin (Fig. 5, lanes *6–8*). ScN_2a cells were grown for 4 d under conditions similar to those described above for the immunoblotting experiments and radiolabeled for 2 h with [^{35}S]methionine. After lysis, PrP immunopurified before SDS-PAGE and autoradiography (Fig. 5, lanes *6–8*). Since no detectable radiolabeled PrP^{Sc} is produced in ScN_2a cells within this time frame (Borchelt et al., 1990, 1992), we did not separate radiolabeled PrP^C from unlabeled PrP^{Sc}. Interestingly, not only did PrP^C not decrease, but it often increased in cells treated with lovastatin and low-fat serum, as

compared to cells incubated with low-fat serum alone. In contrast, less PrP^c could be released by PIPLC from the surface of the lovastatin-treated cells, suggesting that PrP^c might not be available for conversion into PrP^{Sc} in cholesterol-depleted cells (data not shown). Whether this is due to the inaccessibility of cell surface PrP^c to PIPLC, to a reduced export of the protein to the plasma membrane, or to the increased partition of PrP^c into internal recycling compartments in cholesterol-deprived cells remains to be determined. Delays in export of PrP^c to the plasma membrane could result in decreased PrP^{Sc} formation, since it was shown earlier with PIPLC-releasable PrP^c is the precursor to PrP^{Sc} in ScN_2a cells (Borchelt et al., 1992; Caughey and Raymond, 1991). In contrast to these results with PrP^c, the pool of intracellular folate receptor was diminished, rather than increased, in lovastatin-treated MA104 cells (Chang et al., 1992).

Transmembrane Anchorage Inhibits PrP^{Sc} Formation

To appreciate better the role of the cholesterol-rich microdomains in the metabolism of GPI-anchored PrP^c, we sought to uncouple PrP^c from this microenvironment by replacing the GPI anchor by a transmembrane fragment. Data from a previous study suggested that the GPI anchor is dispensable for the structural changes that occur in PrP^{Sc} formation (Rogers et al., 1993); we constructed a hybrid PrP gene in which the GPI attachment signal was replaced with the putative transmembrane and cytoplasmic regions of mouse CD4 (Fig. 6 *A*) (Littman and Gettner, 1987). Proteins anchored through this CD4 fragment cluster on clathrin-coated pits rather than on uncoated regions of the plasma membrane (Keller et al., 1992). To construct the hybrid PrP, we employed the chimeric MHM2PrP gene (Scott et al., 1992) which carries a SHa-specific PrP epitope recognized by the 3F4 mAb (Kascsak et al., 1987) (Fig. 6 *A*). This construction permitted us to discriminate the CD4MHM2PrP from the endogenous MoPrP in ScN_2a cells. Introduction of the 3F4 mAb epitope (Met_{108}-Met_{111}) did not prevent PrP^{Sc} formation when introduced into the GPI-anchored MoPrP (Rogers et al., 1991; Scott et al., 1992).

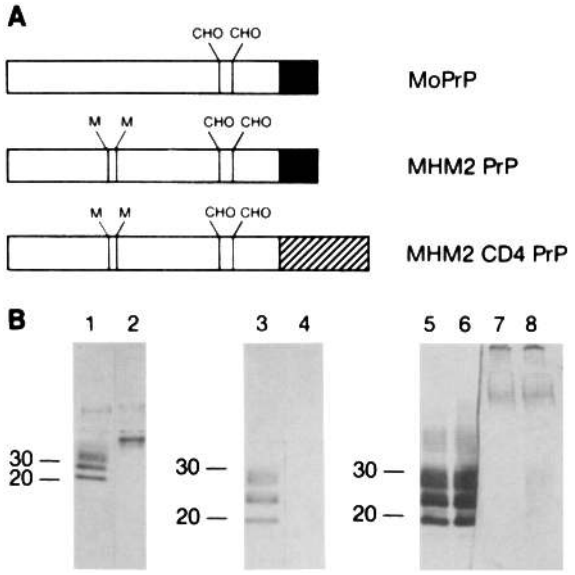

Figure 6. Expression of CD4PrP in ScN_2a cells. (*A*) Map of the MHM2PrP and CD4PrP constructs. (*Full bar*) GPI attachment sequence. (*Hatched bar*) Transmembrane and cytoplasmic sequences from MoCD4. (*B*) ScN_2a cells (lanes *1*, *3*, *5*, and *6*) and ScN_2a cells transfected with the CD4PrP construct (lanes *2*, *4*, *6*, and *8*) were analyzed for PrP^c (lanes *1* and *2*) and PrP^{Sc} (lanes *3–8*) by Western immunoblotting using R073 (lanes *1*, *3*, *5*, and *6*) or 3F4 (lanes *2*, *4*, *7*, and *8*). In lanes *5–8*, PrP^{Sc} was concentrated as follows: 1 ml lysates from a 9-cm plate were subjected to proteolysis (20 μg/ml proteinase K, 37°C, 1 h) followed by a high-speed spin to purify PrP^{Sc}, and a whole plate equivalent was loaded in each lane. 20 μl of the lysates were centrifuged (57,000 *g*, 1 h, 4°C) to separate PrP^c from PrP^{Sc}; supernatants were loaded on lanes *1* and *2* and pellets loaded on lanes *3* and *4*. ScN_2a cells transfected with CD4PrP did not synthesize appreciable amounts of CD4-PrP^{Sc} (lanes *4* and *8*).

We transfected ScN_2a cells with the recombinant CD4-PrP gene and used an uncloned cell population in the subsequent experiments, which was selected by an addition of G418 to the cultures. Western immunoblotting developed with 3F4 confirmed that transfected ScN_2a cells synthesized $CD4PrP^c$ (Fig. 6 *B*, lane *2*). As expected, the M_r of this $CD4PrP^c$ was slightly larger than that of GPI-anchored wtPrP (lane *1*). To determine whether CD4PrP can be converted into PrP^{Sc}, the CD4PrP construct was transfected into ScN_2a cells (lanes *3–8*). No 3F4 reacting PrP^{Sc} signal could be detected in transfected ScN_2a cells (lane *4*) while the control ScN_2a cells were positive with the polyclonal Ab R073, which recognizes wtPrP (lane *3*). To increase the sensitivity of PrP^{Sc} detection in cell lysates, we concentrated PrP^{Sc} ~50-fold by proteolysis followed by ultracentrifugation. In the transfected cells lane, only a very faint protease-resistant signal could be detected with 3F4, even when the lysate from an entire 9-cm dish was loaded onto a single lane (Fig. 6, lane *8*). This signal was specific for the 3F4 epitope since a lysate from untransfected ScN_2a cells yielded no immunoreactive band with this Ab (lane *7*). Since our assay is based on the host cells being persistently infected, thereby providing endogenous prions necessary for the synthesis of PrP^{Sc}, we used the polyclonal antiserum R073 to confirm that these ScN_2a cells were still synthesizing $MoPrP^{Sc}$ at the same level as the original ScN_2a population (lanes *5* and *6*).

We also compared the internalization patterns of GPI-anchored wtPrP and CD4PrP (Fig. 7). ScN_2a cells were labeled at 4°C with R073 Abs or 3F4 mAbs, and then chased for 45 min at either 4 or 37°C. After fixing and permeabilizing the cells, the pattern of PrP Ab internalization was examined by immunofluorescence (Fig. 7 *B*). After the 37°C chase, GPI-anchored wtPrP either remained on the cell surface or was internalized to a compartment near the surface; whereas, CD4PrP was internalized to the perinuclear region. Thus, $CD4PrP^c$ seems to differ from its GPI-anchored counterpart both by its plasma membrane distribution and by its internalization pattern (Keller et al., 1992).

$CD4PrP^c$ Is Soluble in Cold Triton X-100

The purpose of the chimeric CD4PrP was to remove PrP from the cholesterol-rich, Triton X-100 insoluble microenvironment with which GPI anchored PrP^c associates. We employed Triton X-100 solubility to ascertain that the chimeric protein was indeed not associated with these microdomains (Brown and Rose, 1992; Cerneus et al., 1993). First,

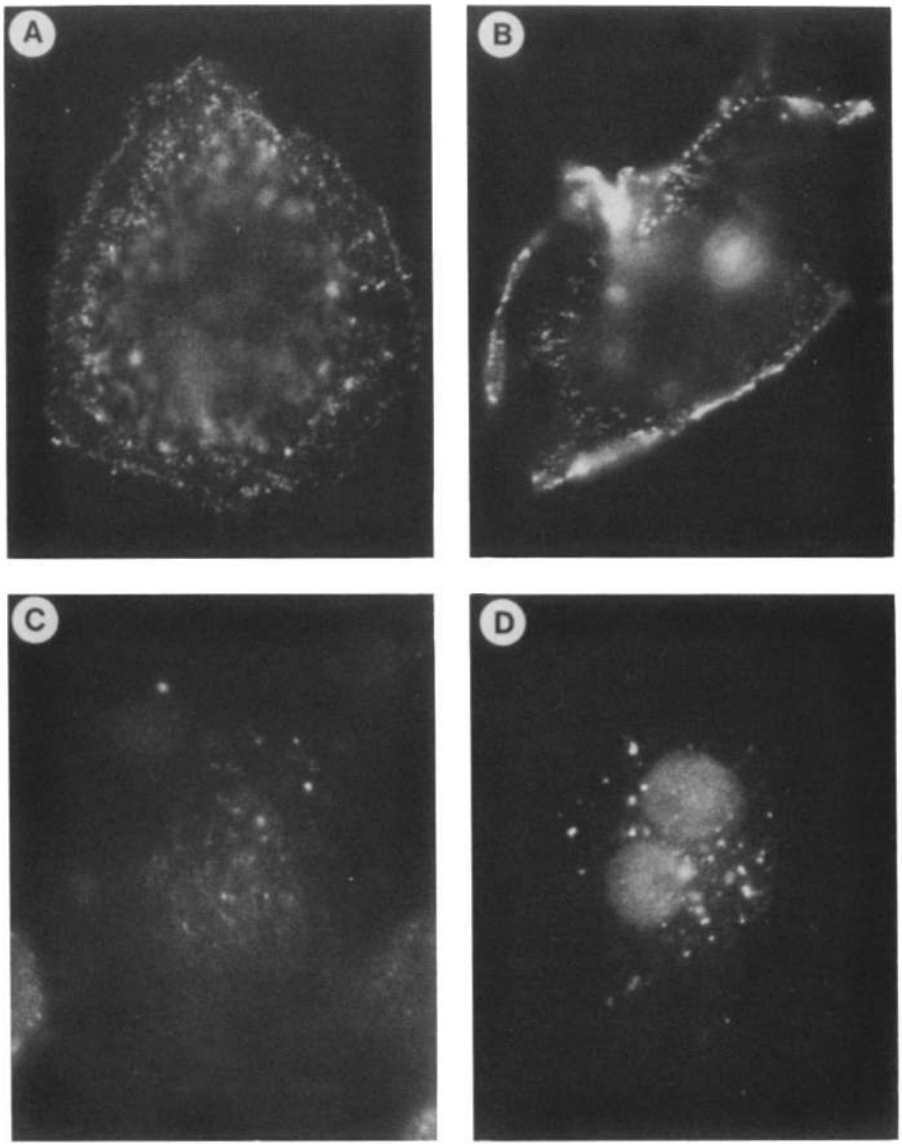

Figure 7. Contrasting localization and internalization of GPI- and CD4-anchored PrP. ScN_2a cells were incubated at 4°C with R073 antiserum (*A* and *B*) and ScN_2a cells expressing CD4HM2-PrP with 3F4 mAb (*C* and *D*), and then chased for 45 min at 4°C (*A* and *C*) or 37°C (*B* and *D*). The cells were then fixed, permeabilized, and the PrP Abs revealed by immunofluorescence. While GPI-anchored PrP^c either remained on the plasma membrane or was internalized within a shallow compartment, the CD4PrP accumulated in the perinuclear region.

we verified that the solubility of GPI-linked wtPrP^c in Triton X-100 is temperature-dependent. ScN_2a cells were radiolabeled for 2 h, and then lysed in 1% Triton X-100 at either 4°C (Fig. 8, lane *1*) or 37°C (lane *2*) or at 4°C in 1% Triton X-100 supplemented with 1% saponin (lane *3*). The lysates were centrifuged at 39,000 *g* for 30 min at either 4°C or 25°C and the supernatants were analyzed by immunoprecipitation and SDS-PAGE. As expected, PrP^c was relatively insoluble in Triton X-100 at 4°C, and saponin increased its solubility arguing that PrP^c is bound to cholesterol-rich domains (Cerneus et al., 1993). In contrast to the GPI-anchored PrP^c, CD4PrP^c was solubilized equally well at 4°C and at 37°C (lanes *4* and *5*), confirming that the recombinant protein is not associated with cholesterol-rich complexes.

We found that ultracentrifugation at 39,000 *g* for 30 min was essential to detect the differential insolubility of PrP^c in cold Triton X-100. These sedimentation conditions are more extreme than those used for MDCK cells and suggest that the cholesterol and glycolipid rich microdomains derived from N_2a cells are either smaller or more buoyant than those from MDCK cells (Brown and Rose, 1992).

Because earlier studies showed that the formation of PrP^{sc} is inhibited by brefeldin A (BFA) (Taraboulos et al., 1992), we examined the effect of BFA on the compartmentalization of PrP^c. When ScN_2a cells were radiolabeled in the presence of BFA (5 μg/ml), PrP^c solubility was found to be similar at 4°C and at 37°C. These results and the finding that the solubilization of PrP^c was unaltered by saponin (Fig. 8, lanes *6–8*), suggest that nascent PrP^c molecules synthesized in the presence of BFA did not associate to the cholesterol-rich environment. Therefore, as in the case of the CD4PrP chimera, we observed a correlation between association of PrP^c with Triton X-100 insoluble membrane domains, and the ability of this PrP^c to be converted into PrP^{sc}.

Discussion

In cells infected with prions, PrP^c has two different meta-

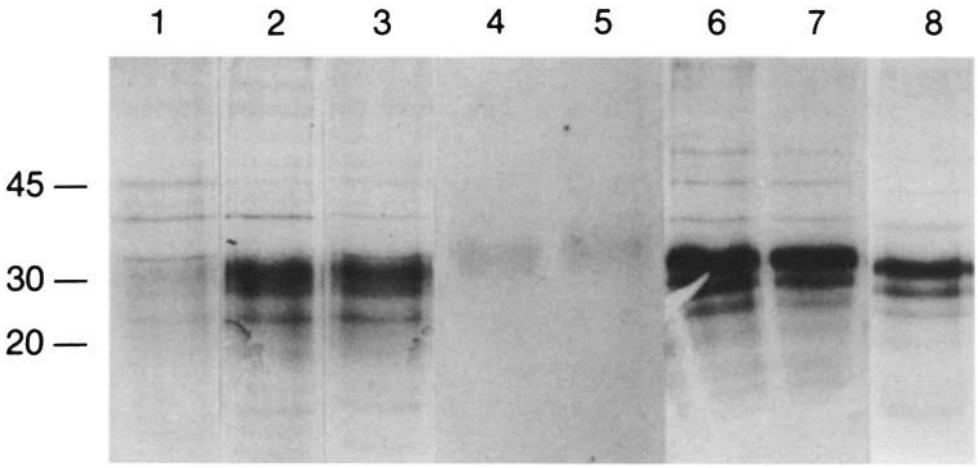

Figure 8. Contrasting solubility of wtPrP and CD4PrP in Triton X-100. Untransfected ScN_2a cells (lanes *1–3*, *6–8*) and ScN_2a cells transfected with the CD4PrP gene (lanes *4–5*) were radiolabeled for 2 h, and then lysed in 1% Triton X-100 either at 37°C (lanes *2*, *5*, and *6*) or at 4°C (lanes *1*, *4*, and *7*), or at 4°C in 1% Triton X-100 + 1% saponin (lanes *3* and *8*). In lanes *6–8*, BFA (5 μg/ml) was included in the labeling medium. The lysates were centrifuged (39,000 *g*, 30 min), and PrP was immunopurified from the supernatants with either R073 (lanes *1–3*, *6–8*) or 3F4 (lanes *4* and *5*). wtMoPrP was almost insoluble in Triton X-100 at 4°C (lane *1*) while CD4PrP was as soluble at 4°C as it was at 37°C.

bolic fates which are mutually exclusive. A minority of PrP^c molecules undergoes a conformational change to become PrP^{Sc} while most of the PrP^c is degraded through a pathway which is indistinguishable from that found in uninfected cells. Our results suggest that both metabolic fates involve events mediated by membranes which are rich in cholesterol.

Multiple lines of experimentation point to relationship between cholesterol-dependent pathways and the metabolism of PrP. First, PrP^{Sc} synthesis was substantially reduced in cells treated with lovastatin while PrP^c levels were unchanged or increased. Since addition of cholesterol together with lovastatin prevented inhibition of PrP^{Sc} synthesis, we surmise that lovastatin exerted its effect through depletion of other mevalonate metabolites. While mevalonate is an obligate precursor for all isoprenoids, studies have shown that sterols are far more sensitive to reduced mevalonate concentration. To provide for non-sterol isoprenoid synthesis, we added 200 μM mevalonate to all lovastatin-treated cells in our experiments. Second, replacing the GPI anchor of PrP with the CD4 transmembrane domain targeted it to clathrin-coated pits and reduced the conversion of PrP^c into PrP^{Sc}. Since truncated PrP^c lacking the GPI anchor addition signal can be converted into PrP^{Sc} but at a diminished level (Kitamoto et al., 1993; Rogers et al., 1993), we surmise that the failure of $CD4PrP^c$ to be transformed into $CD4PrP^{Sc}$ is likely to result from its targeting to clathrin-coated pits instead of cholesterol-rich membrane domains. It will be important to examine additional amino acid sequences which are known to target proteins to clathrin-coated pits in order to determine whether it is the targeting or altered conformation that prevents PrP^{Sc} formation. Third, temperature-dependent solubility in Triton X-100 confirmed the association of GPI-anchored PrP^c with cholesterol- and glycolipid-rich complexes, in contrast to $CD4PrP^c$. Since the degradation intermediate of PrP^c was also GPI anchored to these complexes, as judged by its differential solubility in Triton X-100 and its releasability with PIPLC, it appears that the first step in PrP^c degradation takes place within these cholesterol-rich complexes. Fourth, PrP^c degradation was diminished in cells deprived of cholesterol. Fifth, that cholesterol-rich complexes are involved in PrP^{Sc} synthesis is suggested by the finding that BFA, known to inhibit PrP^{Sc} formation in ScN_2a cells (Taraboulos et al., 1992), prevented the association of PrP^c with detergent-insoluble complexes. The failure of PrP^c to associate with cholesterol-rich domains may provide a mechanism to account for the inhibition of PrP^{Sc} formation by BFA.

PrP^c Degradation

Studies of the turnover of PrP^c are of considerable importance with respect to prion diseases since diminished expression in gene targeted mice prolongs incubation times (Büeler et al., 1993; Prusiner et al., 1993) while overexpression shortens them (Carlson et al., 1994; Prusiner et al., 1990). In older mice overexpression of wtPrP transgenes produced spongiform degeneration of the CNS, a necrotizing myopathy of skeletal muscle, a demyelinating peripheral neuropathy and spontaneous formation of prion infectivity (Westaway et al., 1994). Results from cell culture studies are consistent with earlier investigations which identified an NH_2-terminally truncated molecule labeled PrP^c-II in extracts and partially purified fractions from the brains of Syrian hamsters (Haraguchi et al., 1989; Pan et al., 1992). $SHaPrP^c$-II was thought to be generated by enzymatic cleavage of PrP^c at a site specific for a protease with the specificity of chymotrypsin. For $MoPrP^c$-A present in N_2a cells (Borchelt et al., 1992; Westaway et al., 1987), the most likely cleavage point for a protease with chymotrypsin-like activity is Tyr_{128} since chymotrypsin cleaves preferentially on the carboxyl site of Tyr, Trp, or Phe. Tyr_{128} is conserved in all known species studied, to date (Gabriel et al., 1992). It is interesting to note that in the chicken PrP sequence, the substitution of Phe in position 109 (numbered according to SHaPrP) (Harris et al., 1991) provides an additional cleavage site for chymotrypsin-like proteases in this region, and that cleavage at this site has been reported in N_2a cells transfected with chicken PrP (Harris et al., 1993). These findings taken together argue that it is likely that a chymotryptic protease initiates the degradation of PrP^c by excising a ~9-kD fragment from the NH_2-terminus of PrP^c resulting in the formation of PrP^c-II.

Although the first degradation step of PrP^c seems to occur within detergent insoluble membrane complexes,

whether it takes place on the plasma membrane or requires internalization remains to be determined. At present, it is unknown whether proteases specific for cholesterol-dependent pathways participate in PrP^c degradation. Several GPI-anchored peptidases have been described (Deddish et al., 1990; Hooper et al., 1990). The presence of these peptidases in rafts suggests that other proteases, such as a putative PrP^c-cleaving enzyme, may also be present in these membrane domains. Since $CD4PrP^c$ is not GPI anchored, it seems likely that the degradation of this protein will differ from that of $wtPrP^c$. Several studies have shown that GPI-anchored molecules are endocytosed through different pathways than their transmembrane counterparts (Keller et al., 1992; Yanagishita, 1992).

Whether PrP^c-II can be converted into a truncated form of PrP^{Sc} is unknown. PrP^c-II appears to lack the first putative α-helical domain (H1, codons 109-122) which is likely to be necessary for PrP^{Sc} formation (Gasset et al., 1992). Of note are two familial prion diseases where the patients accumulated truncated PrP^{Sc} molecules within PrP amyloid plaques but in each case these proteins contained the H1 region (Kitamoto et al., 1993; Tagliavini et al., 1991). A truncated PrP gene was constructed in which the signal peptide (codons 1-22) was fused to codons 90-254 to produce a protein similar in length to PrP 27-30 which contains H1. In ScN_2a cells this truncated PrP did acquire the protease resistance which is a hallmark of PrP^{Sc} (Rogers et al., 1993). Studies are in progress to determine if a molecule the size of PrP^c-II can acquire protease resistance in cultured cells and support scrapie infectivity in transgenic mice.

Do Cholesterol-Rich Domains Play a Role in the Formation of PrP^{Sc}?

The formation of PrP^{Sc} is a posttranslational process in which PrP^{Sc} combines with PrP^c to form a transient complex (Prusiner et al., 1990; Scott et al., 1993). The conversion of PrP^c into PrP^{Sc} involves a profound conformational change where the primary event seems to be the acquisition of a structure rich in β-sheet (Pan et al., 1993). PrP^{Sc} appears to serve as a "template" for the conversion of PrP^c which may explain, at least in part, the apparent diversity of prions which has often been referred to as "strains." Whether each strain represents a distinct conformer of PrP^{Sc} which exhibits a particular incubation time and pattern of PrP^{Sc} deposition in a specific host remains to be established (Carlson et al., 1994; DeArmond et al., 1993; Prusiner, 1991). Our results argue that PrP^{Sc} formation occurs in cholesterol-rich, detergent-insoluble domains that contain GPI-anchored PrP^c. The insolubility of PrP^{Sc} in nondenaturing detergents such as Triton X-100 (Meyer et al., 1986) has precluded demonstrating attachment of PrP^{Sc} in these cholesterol-rich, detergent-insoluble domains. The presumed transient nature of the PrP^c/PrP^{Sc} complexes may also make detection of PrP^{Sc} in this compartment difficult. While immunoelectron microscopy has localized PrP^{Sc} primarily to lysosomes in cultured cells, we cannot rule out the possibility of small amounts of PrP^{Sc} in other compartments (McKinley et al., 1991).

Whether or not cholesterol-rich membrane domains promote the formation of PrP^{Sc} by concentrating PrP^c to high surface density remains to be established. Caveolar GPI-anchored folate receptor is very densely packed: 30,000 molecules/μm^2 in MA104 cells (Rothberg et al., 1990*a*). If cholesterol-rich domains were to concentrate GPI-anchored PrP^c either on the plasma membrane or in other sites, they could provide a propitious environment for the formation of PrP^{Sc}. Alternatively, cholesterol-rich domains might function by targeting PrP^c to other compartments where PrP^{Sc} is formed. Of note, an extensive caveolar recycling of cholesterol-rich domains from the PM to the TGN is likely to exist, since transport of the influenza HA to the PM proceeds in MDCK cells even when the viral infection halts the synthesis of endogenous proteins (Wandinger-Ness et al., 1990). In the case of the folate receptor, caveolae are engaged in the recycling of this GPI-anchored protein before becoming acidified (Anderson et al., 1992). It is interesting to note that PrP^{Sc} formation is insensitive to lysosomotropic amines (Caughey et al., 1991; Taraboulos et al., 1992) whereas receptor-mediated folate uptake is inhibited by NH_4Cl.

Subcellular Sites of PrP^{Sc} Formation

The studies described here coupled with earlier reports begin to refine our view of PrP^{Sc} formation at the subcellular level. It seems likely that PrP^{Sc} is formed in a compartment bounded by cholesterol-rich, detergent-insoluble membrane domains. Whether these domains might anchor other proteins that facilitate the conversion of PrP^c into PrP^{Sc} is unknown (Raeber et al., 1992). Considerable evidence argues that the conversion of PrP^c into PrP^{Sc} involves the posttranslational unfolding and refolding of PrP into a pathogenic conformer (Pan et al., 1993). Attempts to identify a chemical event that triggers the acquisition of this pathogenic conformation have been unrewarding, to date (Stahl et al., 1993). Transgenetic studies argue that the production of PrP^{Sc} requires formation of an intermediate complex in which PrP^{Sc} and PrP^c interact (Prusiner et al., 1990; Scott et al., 1993). The results of other transgenic mouse studies argue that an additional host protein participates in the generation of PrP^{Sc} (Telling et al., 1994).

Whether the subcellular compartment(s) in which PrP^{Sc} is formed is the same in which the initial degradation of PrP^c to a 17-kD polypeptide (PrP^c-II) occurs remains to be established. That both the formation of PrP^{Sc} and the initial degradation of PrP^c occur in the same non-acidic compartment bounded by cholesterol-rich membranes is an attractive hypothesis that warrants further study. Since the formation of PrP^{Sc} uses full-length PrP^c, such a compartment would be a metabolic branch point where the fate of PrP^c is determined.

The minimal formation of $CD4PrP^{Sc}$ is in accord with the low levels of truncated PrP^{Sc} which appears to lack a GPI anchor (Rogers et al., 1993). These results taken together with the inhibition of PrP^{Sc} formation by cholesterol depletion support the hypothesis that GPI anchorage, probably functioning in concert with cholesterol-dependent pathways, is instrumental in the formation of PrP^{Sc} in ScN_2a cells. Such conclusions must be tempered by the results of studies which suggest that GPI-anchored proteins may not be constitutively bound to caveolae, but rather associate with these structures when multimerized, for instance, with divalent antibodies (Mayor et al., 1994). Since the PrP antibodies are divalent, it is possible that the behavior of PrP^c displayed in Fig. 3 was induced by cross-linking with α-PrP antibodies.

However, the results clearly indicate that wtPrP^{c} was internalized differently under the conditions of the experiments than chimeric CD4PrP^{c} which was targeted to clathrin-coated pits.

It seems likely that as the roles of caveolae and cholesterol-rich membranous microdomains become better understood, new tools will become available to decipher the subcellular events that feature in prion replication. If PrP^{Sc} is formed in a single subcellular compartment, then isolation of those organelles might facilitate development of a system for the in vitro formation of PrP^{Sc} and the identification of proteins which function in this process (Telling et al., 1994).

This work was supported by research grants from the National Institutes of Health and a gift from the Sherman Fairchild Foundation.

Received for publication 6 April 1994 and in revised form 19 December 1994.

References

Anderson, R. G., B. A. Kamen, K. G. Rothberg, and S. W. Lacey. 1992. Potocytosis: sequestration and transport of small molecules by caveolae. *Science (Wash. DC).* 255:410–411.

Anderson, R. G. W. 1993. Caveolae: where incoming and outgoing messenger meet. *Proc. Natl. Acad. Sci. USA.* 90:10909–10913.

Barry, R. A., and S. B. Prusiner. 1986. Monoclonal antibodies to the cellular and scrapie prion proteins. *J. Infect. Dis.* 154:518–521.

Barry, R. A., M. T. Vincent, S. B. H. Kent, L. E. Hood, and S. B. Prusiner. 1988. Characterization of prion proteins with monospecific antisera to synthetic peptides. *J. Immunol.* 140:1188–1193.

Borchelt, D. R., M. Scott, A. Taraboulos, N. Stahl, and S. B. Prusiner. 1990. Scrapie and cellular prion proteins differ in their kinetics of synthesis and topology in cultured cells. *J. Cell Biol.* 110:743–752.

Borchelt, D. R., A. Taraboulos, and S. B. Prusiner. 1992. Evidence for synthesis of scrapie prion proteins in the endocytic pathway. *J. Biol. Chem.* 267:16188–16199.

Brown, D. A., and J. K. Rose. 1992. Sorting of GPI-anchored proteins to glycolipid-enriched membrane subdomains during transport to the apical cell surface. *Cell.* 68:533–544.

Büeler, H., A. Aguzzi, A. Sailer, R.-A. Greiner, P. Autenried, M. Aguet, and C. Weissmann. 1993. Mice devoid of PrP are resistant to scrapie. *Cell.* 73:1339–1347.

Butler, D. A., M. R. D. Scott, J. M. Bockman, D. R. Borchelt, A. Taraboulos, K. K. Hsaio, D. T. Kingsbury, and S. B. Prusiner. 1988. Scrapie-infected murine neuroblastoma cells produce protease-resistant prion proteins. *J. Virol.* 62:1558–1564.

Carlson, G. A., C. Ebeling, S.-L. Yang, G. Telling, M. Torchia, D. Groth, D. Westaway, S. J. DeArmond, and S. B. Prusiner. 1994. Prion isolate specified allotypic interactions between the cellular and scrapie prion proteins in congenic and transgenic mice. *Proc. Natl. Acad. Sci. USA.* 91:5690–5694.

Caughey, B., and G. J. Raymond. 1991. The scrapie-associated form of PrP is made from a cell surface precursor that is both protease- and phospholipase-sensitive. *J. Biol. Chem.* 266:18217–18223.

Caughey, B., R. E. Race, D. Ernst, M. J. Buchmeier, and B. Chesebro. 1989. Prion protein biosynthesis in scrapie-infected and uninfected neuroblastoma cells. *J. Virol.* 63:175–181.

Caughey, B., G. J. Raymond, D. Ernst, and R. E. Race. 1991. N-terminal truncation of the scrapie-associated form of PrP by lysosomal protease(s): implications regarding the site of conversion of PrP to the protease-resistant state. *J. Virol.* 65:6597–6603.

Cerneus, D. P., E. Ueffing, G. Posthuma, G. J. Strous, and A. van der Ende. 1993. Detergent insolubility of alkalaine phosphatase during biosynthetic transport and endocytosis. Role of cholesterol. *J. Biol. Chem.* 268:3150–3155.

Chang, W. J., K. G. Rothberg, B. A. Karman, and R. G. Anderson. 1992. Lowering the cholesterol content of MA104 cells inhibits receptor-mediated transport of folate. *J. Cell Biol.* 118:63–69.

Cinek, T., and V. Horejsi. 1992. The nature of large noncovalent complexes containing glycosyl-phosphatidylinositol-anchored membrane glycoproteins and protein tyrosine kinases. *J. Immunol.* 149:2262–2270.

DeArmond, S. J., S.-L. Yang, A. Lee, R. Bowler, A. Taraboulos, D. Groth, and S. B. Prusiner. 1993. Three scrapie prion isolates exhibit different accumulation patterns of the prion protein scrapie isoform. *Proc. Natl. Acad. Sci. USA.* 90:6449–6453.

Deddish, P. A., R. A. Skidgel, V. B. Kriho, X. Y. Li, R. P. Becker, and E. G. Erdos. 1990. Carboxypeptidase M in Madin-Darby canine kidney cells. Evidence that carboxypeptidase M has a phosphatidylinositol glycan anchor. *J. Biol. Chem.* 265:15083–15089.

Gabriel, J.-M., B. Oesch, H. Kretzschmar, M. Scott, and S. B. Prusiner. 1992. Molecular cloning of a candidate chicken prion protein. *Proc. Natl. Acad. Sci. USA.* 89:9097–9101.

Gasset, M., M. A. Baldwin, D. Lloyd, J.-M. Gabriel, D. M. Holtzman, F. Cohen, R. Flettrick, and S. B. Prusiner. 1992. Predicted α-helical regions of the prion protein when synthesized as peptides form amyloid. *Proc. Natl. Acad. Sci. USA.* 89:10940–10944.

Giloh, H., and J. W. Sedat. 1982. Fluorescence microscopy: reduced photobleaching of rhodamine and fluorescein protein conjugates by N-propyl gallate. *Science (Wash. DC).* 217:1252–1254.

Goldstein, J. L., S. K. Basu, and M. S. Brown. 1983. Receptor mediated endocytosis of low density lipoprotein in cultured cells. *Methods Enzymol.* 98:241–260.

Haraguchi, T., S. Fisher, S. Olofsson, T. Endo, D. Groth, A. Tarantino, D. R. Borchelt, D. Teplow, L. Hood, A. Burlingame, et al., 1989. Asparagine-linked glycosylation of the scrapie and cellular prion proteins. *Arch. Biochem. Biophys.* 274:1–13.

Harris, D. A., M. T. Huber, P. van Dijken, S. Shyng, B. T. Chait, and R. Wang. 1993. Processing of a cellular prion protein: identification of N- and C-terminal cleavage sites. *Biochemistry.* 32:1009–1016.

Harris, D. A., D. L. Falls, F. A. Johnson, and G. D. Fischbach. 1991. A prion-like protein from chicken brain copurifies with an acetylcholine receptor-inducing activity. *Proc. Natl. Acad. Sci. USA.* 88:7664–7668.

Heider, J. G., and R. L. Boyett. 1978. The picomole determination of free and total cholesterol in cells in culture. *J. Lipid Res.* 19:514–518.

Hooper, N. M., and A. Bashir. 1991. Glycosyl-phosphatidylinositol-anchored membrane proteins can be distinguished from transmembrane polypeptide-anchored proteins by differential solubilization and temperature-induced phase separation in Triton X-114. *Biochem. J.* 280:745–751.

Hooper, N. M., J. Hryszko, and A. J. Turner. 1990. Purification and characterization of pig kidney aminopeptidase P. A glycosyl-phosphatidylinositol-anchored ectoenzyme. *Biochem. J.* 267:509–515.

Kascsak, R. J., R. Rubenstein, P. A. Merz, M. Tonna-DeMasi, R. Fersko, R. I. Carp, H. M. Wisniewski, and H. Diringer. 1987. Mouse polyclonal and monoclonal antibody to scrapie-associated fibril proteins. *J. Virol.* 61: 3688–3693.

Keller, G. A., M. W. Siegel, and I. W. Caras. 1992. Endocytosis of glycophospholipid-anchored and transmembrane forms of CD4 by different endocytic pathways. *EMBO (Eur. Mol. Biol. Organ.) J.* 11:863–874.

Kitamoto, T., M. Ohta, K. Doh-ura, S. Hitoshi, Y. Terao, and J. Tateishi. 1993. Novel missense variants of prion protein in Creutzfeldt-Jakob disease or Gerstmann-Sträussler syndrome. *Biochem. Biophys. Res. Commun.* 191:709–714.

Kocisko, D. A., J. H. Come, S. A. Priola, B. Chesebro, G. J. Raymond, P. T. Lansbury, Jr., and B. Caughey. 1994. Cell-free formation of protease-resistant prion protein. *Nature (Lond.).* 370:471–474.

Laemmli, U. K. 1970. Cleavage of structural proteins during the assembly of the head of bacteriophage T-4. *Nature (Lond.).* 227:680–685.

Langan, T. J., and J. J. Volpe. 1986. Obligatory relationship between the sterol biosynthetic pathway and DNA synthesis and cellular proliferation in glial primary cultures. *J. Neurochem.* 46:1283–1291.

Littman, D. R., and S. N. Gettner. 1987. Unusual intron in the immunoglobulin domain of the newly isolated murine CD4(L3T4) gene. *Nature (Lond.).* 325:453–455.

Mayor, S., K. G. Rothberg, and F. R. Maxfield. 1994. Sequestration of GPI-anchored proteins in caveolae triggered by cross-linking. *Science (Wash. DC).* 264:1948–1951.

McKinely, M. P., A. Taraboulos, L. Kenaga, D. Serban, A. Stieber, S. J. DeArmond, S. B. Prusiner, and N. Gonatas. 1991. Ultrastructural localization of scrapie prion proteins in cytoplasmic vesicles of infected cultured cells. *Lab. Invest.* 65:622–630.

Meyer, R. K., M. P. McKinley, K. A. Bowman, M. B. Braunfield, R. A. Barry, and S. B. Prusiner. 1986. Separation and properties of cellular and scrapie prion proteins. *Proc. Natl. Acad. Sci. USA.* 83:2310–2314.

Pan, K.-M., M. Baldwin, J. Nguyen, M. Gasset, A. Serban, D. Groth, I. Mehlhorn, Z. Huang, R. J. Fletterick, F. E. Cohen, and S. B. Prusiner. 1993. Conversion of α-helices into β-sheets features in the formation of the scrapie prion proteins. *Proc. Natl. Acad. Sci. USA.* 90:10962–10966.

Pan, K.-M., N. Stahl, and S. B. Prusiner. 1992. Purification and properties of the cellular prion protein from Syrian hamster brain. *Protein Sci.* 1:1343–1352.

Prusiner, S. B., 1991. Molecular biology of prion diseases. *Science (Wash. DC).* 252:1515–1522.

Prusiner, S. B., D. Groth, A. Serban, R. Koehler, D. Foster, M. Torchia, D. Burton, S.-L. Yang, and S. J. DeArmond. 1993. Ablation of the prion protein (PrP) gene in mice prevents scrapie and facilitates production of anti-PrP antibodies. *Proc. Natl. Acad. Sci. USA.* 90:10608–10612.

Prusiner, S. B., M. P. McKinley, K. A. Bowman, D. C. Bolton, P. E. Bendheim, D. F. Groth, and G. G. Glenner. 1983. Scrapie prions aggregate to form amyloid-like birefringent rods. *Cell.* 35:349–358.

Pursiner, S. B., M. Scott, D. Foster, K.-M. Pan, D. Groth, C. Mirenda, M. Torchia, S.-L. Yang, D. Serban, G. A. Carlson, et al. 1990. Transgenetic studies implicate interactions between homologous PrP isoforms in scrapie prion replication. *Cell.* 63:673–686.

Raeber, A. J., D. R. Borchelt, M. Scott, and S. B. Prusiner. 1992. Attempts to convert the cellular prion protein into the scrapie isoform in cell-free systems. *J. Virol.* 66:6155–6163.

Rogers, M., D. Serban, T. Gyuris, M. Scott, T. Torchia, and S. B. Prusiner. 1991. Epitope mapping of the Syrian hamster prion protein utilizing chimeric and mutant genes in a vaccinia virus expression system. *J. Immunol.* 147:3568–3574.

Rogers, M., A. Taraboulos, M. Scott, D. Borchelt, D. Serban, T. Gyuris, and S. B. Prusiner. 1992. Modification and expression of prion proteins in cultured cells. *In* Prion Diseases of Humans and Animals. S. B. Prusiner, J. Collinge, J. Powell, and B. Anderton, editors. Ellis Horwood, London. 457–469.

Rogers, M., F. Yehiely, M. Scott, and S. B. Prusiner. 1993. Conversion of truncated and elongated prion proteins into the scrapie isoform in cultured cells. *Proc. Natl. Acad. Sci. USA.* 90:3182–3186.

Rothberg, K. G., Y. Ying, J. F. Kolhouse, B. A. Kamen, and R. G. W. Anderson. 1990*a*. The glycophospholipid linked folate receptor internalizes folate without entering the clathrin coated pit endocytic pathway. *J. Cell Biol.* 110:637–649.

Rothberg, K. G., Y. S. Ying, B. A. Kamen, and R. G. Anderson. 1990*b*. Cholesterol controls the clustering of the glycophospholipid-anchored membrane receptor for 5-methyltetrahydrofolate. *J. Cell Biol.* 111:2931–2938.

Safar, J., P. P. Roller, D. C. Gajdusek, and C. J. Gibbs, Jr. 1993. Conformational transitions, dissociation, and unfolding of scrapie amyloid (prion) protein. *J. Biol. Chem.* 268:20276–20284.

Scott, M. R., R. Köhler, D. Foster, and S. B. Prusiner. 1992. Chimeric prion protein expression in cultured cells and transgenic mice. *Protein Sci.* 1: 986–997.

Scott, M., D. Groth, D. Foster, M. Torchia, S.-L. Yang, S. J. DeArmond, and S. B. Prusiner. 1993. Propagation of prions with artificial properties in transgenic mice expressing chimeric PrP genes. *Cell.* 73:979–988.

Serban, D., A. Taraboulos, S. J. DeArmond, and S. B. Prusiner. 1990. Rapid detection of Cruetzfeldt-Jakob disease and scrapie prion proteins. *Neurology.* 40:110–117.

Shyng, S.-L., J. E. Heuser, and D. A. Harris. 1994. A glycolipid-anchored prion protein is endocytosed via clathrin-coated pits. *J. Cell Biol.* 125: 1239–1250.

Simons, K., and G. van Meer. 1988. Lipod sorting in epithelial cells. *Biochemistry.* 27:6197–6202.

Stahl, N., M. A. Baldwin, D. B. Teplow, L. Hood, B. W. Gibson, A. L. Burlingame, and S. B. Prusiner. 1993. Structural analysis of the scrapie prion protein using mass spectrometry and amino acid sequencing. *Biochemistry.* 32:1991–2002.

Stahl, N., D. R. Borchelt, K. Hsiao, and S. B. Prusiner. 1987. Scrapie prion protein contains a phosphatidylinositol glycolipid. *Cell.* 51:229–240.

Tagliavini, F., F. Prelli, J. Ghisto, O. Bugiani, D. Serban, S. B. Prusiner, M. R. Farlow, B. Ghetti, and B. Frangione. 1991. Amyloid protein of Gerstmann-Sträussler-Scheinker disease (Indiana kindred) is an 11-kD fragment of prion protein with an N-terminal glycine at codon 58. *EMBO (Eur. Mol. Biol. Organ). J.* 10:513–519.

Taraboulos, A., A. J. Raeber, D. R. Borchelt, D. Serban, and S. B. Prusiner. 1992. Synthesis and trafficking of prion proteins in cultured cells. *Mol. Biol. Cell.* 3:851–863.

Taraboulos, A., M. Rogers, D. R. Brochelt, M. P. McKinley, M. Scott, D. Serban, and S. B. Prusiner. 1990*a*. Acquisition of protease resistance by prion proteins in scrapie-infected cells does not require asparagine-linked glycosylation. *Proc. Natl. Acad. Sci. USA.* 87:8262–8266.

Taraboulos, A., D. Serban, and S. B. Prusiner. 1990*b*. Scrapie prion proteins accumulate in the cytoplasm of persistently infected cultured cells. *J. Cell Biol.* 110:2117–2132.

Telling, G. C., M. Scott, D. Foster, S.-L. Yang, M. Torchia, K. C. L. Sidle, J. Collinge, S. J. DeArmond, and S. B. Prusiner. 1994. Transmission of Creutzfeldt-Jakob disease from humans to transgenic mice expressing chimeric human-mouse prion protein. *Proc. Natl. Acad. Sci. USA.* 91:9936–9940.

Wandinger-Ness, A., M. K. Bennett, C. Antony, and K. Simons. 1990. Distinct transport vesicles mediate the delivery of plasma membrane proteins to the apical and basolateral domains of MDCK cells. *J. Cell Biol.* 111: 987–1000.

Westaway, D., P. A. Goodman, C. A. Mirenda, M. P. McKinley, G. A. Carlson, and S. B. Prusiner. 1987. Distinct prion proteins in short and long scrapie incubation period mice. *Cell.* 51:651–662.

Westaway, D., S. J. DeArmond, J. Cayetano-Canlas, D. Groth, D. Foster, S.-L. Yang, M. Torchia, G. A. Carlson, and S. B. Prusiner. 1994. Degeneration of skeletal muscle, peripheral nerves, and the central nervous system in transgenic mice overexpressing wild-type prion proteins. *Cell.* 76: 117–129.

Yanagishita, M. 1992. Glycosylphosphatidylinositol-anchored and core protein-intercalated heparan sulfate proteolgycans in rat ovarian granulosa cells have distinct secretory, endocytotic, and intracellular degradative pathways. *J. Biol. Chem.* 267:9505–9511.

Ying, Y.-S., R. G. W. Anderson, and K. G. Rothberg. 1992. Each caveola contains multiple glycosyl-phosphatidylinositol-anchored membrane proteins. *Cold Spring Harb. Symp. Quant. Biol.* 57:593–604.